Evidence of a Cholesteric Liquid Crystalline Phase in Natural Silk Spinning Processes

P. Jeanene Willcox and Samuel P. Gido*

Department of Polymer Science and Engineering, University of Massachusetts−Amherst, Amherst, Massachusetts 01003-4530

Wayne Muller and David L. Kaplan

U.S. Army Natick Research and Development Center, Biotechnology Division, Natick, Massachusetts 01760-5020

Received April 18, 1996[⊗]

ABSTRACT: A look inside the silk spinning process along the length of a silk gland has been achieved by the cryogenic quenching and subsequent microtoming of live silk-spinning animals, *Nephila clavipes* (spider) and *Bombyx mori* (silkworm). Observations made using transmission electron microscopy, electron diffraction and atomic force microscopy indicate a cholesteric liquid crystalline phase of aqueous silk fibroin in the early duct portion of the major silk-producing gland in both species. Transmission electron microscopy (TEM) and atomic force microscopy (AFM) provide evidence for the cholesteric intermediate phase. The fracture surface produced by the diamond microtoming knife follows the twist of the director field, yielding thin sections with an undulating surface topography which produces a characteristic banding, on the order of 200−600 nm, in TEM and AFM images. Electron diffraction results also support the picture of the aqueous silk existing as a cholesteric at an intermediate stage in the spinning process.

1. Introduction

The exceptional mechanical properties of natural silk fibers and the efficiency of silk spinning in nature have produced an effort to understand the natural silk process as it proceeds from the biosynthesis of the silk protein (fibroin) to the spinning of the fiber. However, many aspects of the process still elude investigators. Natural silk fibers are semicrystalline, with a high degree of molecular orientation. These natural fibers are formed through a relatively low pressure, room temperature process, and although silk is spun from an aqueous solution, the resulting fiber is water insoluble, due to an irreversible phase change during the spinning process. A liquid crystalline intermediate phase of silk in aqueous solution, with a high degree of precrystalline molecular orientation, has long been postulated and could explain the ability of this natural process to transform a molecule which exists as a random coil in aqueous solution into an insoluble, highly oriented fiber.

Evidence that has been cited to support the presence of a liquid crystalline phase has included optical birefringence of the contents of the silk glands, the low viscosity of concentrated fibroin solution, a low critical shear rate for inducing crystallization in aqueous fibroin, and the calculated low draw ratios necessary for production of uniaxially aligned fibrous structures from silk fibroin.[1−4] The most significant optical microscopy evidence of liquid crystallinity in silk solutions was presented by Viney *et al.*,[4,5] who observed schlieren textures and extinction bands due to $+1/2$ disclinations in silk secretions extracted from the silk glands of both *N. clavipes* and *B. mori*. These studies showed that it is possible for silk solutions to form nematic liquid crystalline phases when confined between a glass slide and coverslip, and after the evaporation of water. However, these observations do not necessarily represent the structure present within the gland under natural spinning conditions.

2. Experimental Section

We have been able to directly observe and image a cholesteric liquid crystalline phase of silk fibroin as it exists within the silk-producing glands of two silk-spinning species, *Nephila clavipes* (spider) and *Bombyx mori* (silkworm). This observation is accomplished by cryogenically quenching the animals during the spinning process and then analyzing the morphology of the material within the silk gland using transmission electron microscopy (TEM), electron diffraction, and atomic force microscopy (AFM). For our investigation, live specimens of *N. clavipes* and *B. mori* were quenched in liquid propane while in the process of spinning silk. Measurements utilizing a fine thermocouple inside a representative specimen's body indicate that our quenching process completely immobilizes the contents of the silk gland in a fraction of a second. Since silk fibroin is a high molecular weight protein[6] (350 000 g/mol) and the quenching process is very rapid, it is likely that we are able to observe the structure of intermediate stages in silk spinning. We cannot exclude the possibility that the quenching process may perturb the structures we wish to observe, but previous workers have performed similar quenching experiments on silk solutions *in vitro* and found no change in the conformation of the molecule.[7]

After quenching, the frozen abdomen of the spider, the location of the major ampullate gland, and the head of the silkworm, the location of the anterior region of the silk gland, were mounted in a cryoultramicrotome and thin sections, 500−1000 Å thick, were cut for observation. Figure 1 shows a schematic representation of the glands of each species. The microtomed sections were maintained at cryogenic temperatures throughout the preparation, transfer, and observation processes. Bright-field TEM images and electron diffraction patterns were collected using both a JEOL 100CX TEM and a JEOL 200FX TEM. After the sections were freeze-dried within the high vacuum of the microscope chamber, room temperature observation of the microstructure using a Topometrix 2010X AFM was possible.

3. Results and Discussion

For both silk-spinning species, the silk protein is synthesized by epithelial cells in the lining of the tail or secretory portion of the gland and then stored in a 20−30% aqueous solution in the ampulla (*N. clavipes*) or reservoir (*B. mori*) portion of the gland. When the silk spinning process begins, the silk solution proceeds

* To whom correspondence should be addressed.
[⊗] Abstract published in *Advance ACS Abstracts,* June 15, 1996.

S0024-9297(96)00588-8 CCC: $12.00

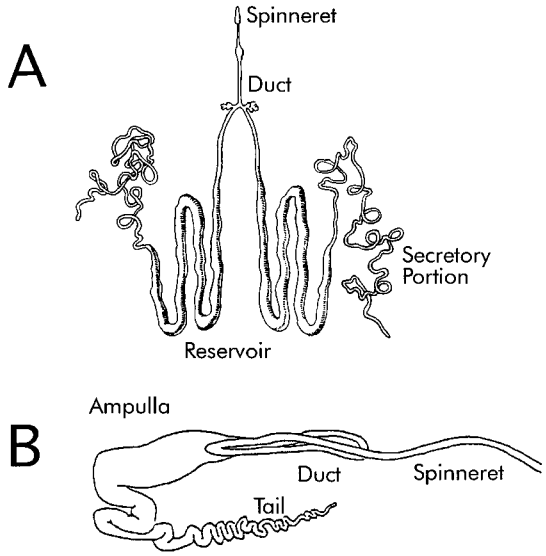

Figure 1. Schematic representations of the silk glands studied: (A) the silk gland of *B. mori*; (B) the major ampullate gland of *N. clavipes*. Cryomicrotomed samples of the glands were taken from the duct regions of both species.

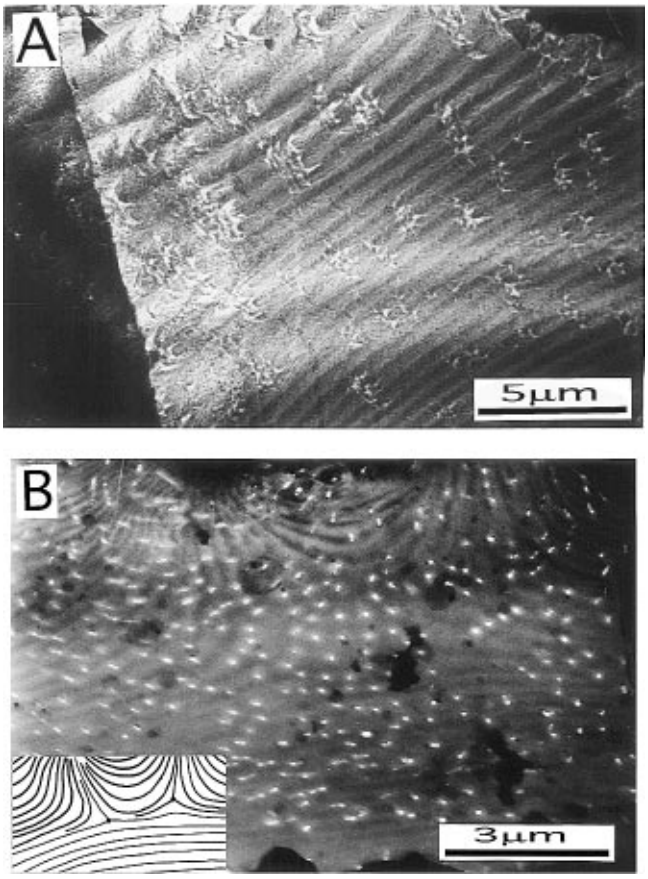

Figure 2. Bright-field TEM images of sections taken from the silk gland ducts of *B. mori* (A) and *N. clavipes* (B). A banded texture is observed with a repeat distance of about 250 nm for the spider and 600 nm for the silkworm. The presence of two λ lines can be seen in the TEM image in (B).

into the duct and, finally, through the spinneret as a molecularly aligned semicrystalline fiber. Figure 2A shows a TEM image of a cross section of the duct region of the silk gland for *B. mori*, exhibiting a banded texture. The banding observed when imaging a cholesteric liquid crystal compound in the glassy state arises due to mass−thickness variations of the sample. When microtoming of a solid-phase cholesteric occurs parallel to the helical axis, a sinusoidal surface topography is produced due to the preferential crack propagation along the spatially varying director field.[8,9] The thin sections are bounded by two of these sinusoidal fracture surfaces, and the phase relationship between the top and bottom periodic surface topographies results in thickness variations which are maximized when the two surfaces are 180° out of phase. When such a sample is viewed in the TEM perpendicular to the helical axis of twist, banded bright-field image contrast arises from thicker regions of enhanced electron scattering power that appear dark, juxtaposed with thinner regions which appear lighter.[10] The exact nature of the periodically varying fracture surface is more clearly elucidated through the use of AFM. Figure 3 shows AFM topography images of a *N. clavipes* sample taken from the duct of the silk gland. A line-trace analysis of the surface topography shows that the fracture of the microtomed sample varies sinusoidally.

The observation of characteristic defect textures (Figure 2B) supports the analysis that the banding seen is the result of a cholesteric liquid crystalline phase. Disclination lines, such as λ lines and $\lambda_+\lambda_-$ pairs, produce the characteristic fingerprint textures observed in bulk cholesteric liquid crystalline materials.[11] It is especially important to note that the observation of these defects precludes the possibility that the banding seen with the TEM is the result of microtoming chatter or other artifacts.[12] The appearance of holes on the order of 100 nm are left by ice crystals which are formed during quenching in liquid nitrogen and sublime away during observation under high vacuum.[13] The disruption of the structure caused by these small holes is minimal, and they can be eliminated altogether (as in Figure 2A) by quenching in liquid propane, a more efficient cryogen.

In order to obtain more quantitative structural information, several series of electron diffraction experiments were conducted on microtomed sections taken from *B. mori*. Correlation between the electron diffraction patterns and the morphological features observed with TEM imaging was accomplished by pairing diffraction patterns with images taken using the defocused central spot of the electron diffraction pattern. Such an image is oriented with respect to the diffraction pattern in our microscope and consists only of the region of sample contributing to the diffraction pattern. Due to the extreme beam sensitivity of the silk phases, low-dose electron diffraction techniques were employed, and diffraction patterns, as well as defocused images, were recorded on ultrasensitive X-ray film (Kodak DEF-5). Figure 4 shows two electron diffraction patterns and their corresponding defocused images. The banded texture is evident in the defocused images. The diffraction patterns show three main reflections: (i) spots on the inner ring that are perpendicular to the banded texture in the defocus image; (ii) a set of arcs inside the inner ring with a second-order set twice the distance out, both of which are parallel to the banded texture; and (iii) a set of arcs just outside the inner ring, also parallel to the banding.

Analysis of the diffraction information is commensurate with the picture of the silk existing as a cholesteric liquid crystal. Figure 5 shows a schematic of the diffraction experiment geometry and the corresponding reciprocal lattice. When the electron beam enters the sample perpendicular to the helical axis of the cholesteric, it is then parallel to the planes which contain the

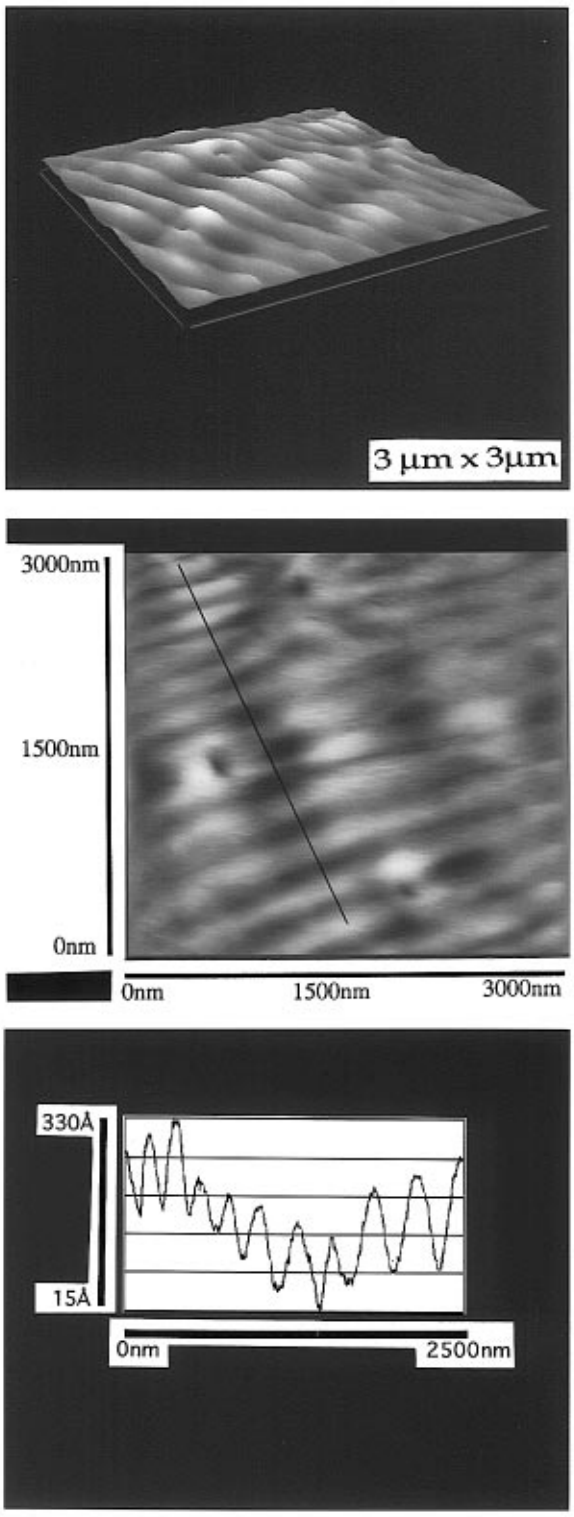

Figure 3. Data from a 3 μm × 3 μm AFM surface scan of the silk gland section from *N. clavipes*. The results of a line trace show that the sinusoidal fracture surface has an average periodicity of 270 nm and an average peak to valley height of 13 nm. This periodicity agrees well with that found for the banding of the spider sample in the TEM.

molecular directors. The average spacing of the mesogenic units along the helical axis direction produces two distinct reflections along this axis. The rings in the *hk*0 plane correspond to spacings within each layer of the cholesteric, such as the interchain spacing between the molecules, or rods, and the monomer unit repeat along the chains. Because of the twisting of the director, these reflections sweep out rings in reciprocal space. In an electron diffraction experiment in which the beam is impinging the sample perpendicular to the twist axis of the cholesteric as shown in Figure 5A, the intersection of the reciprocal lattice with the Ewald sphere produces a diffraction pattern with spots and arcs like that in Figure 4A. Tilting of the sample away from this orientation, Figure 5B, reduces the intensity of the spots (i) and increases the intensity of arcs, (ii) and (iii). The diffraction pattern in Figure 4B clearly shows this effect. The corresponding defocused image, Figure 4B*, has a distinctly different appearance from the image, Figure 4A*, corresponding to the pattern with spots (i). This difference in appearance is a direct result of different sample tilt with respect to the electron beam. The twisted plywood model shown schematically in Figure 6 allows one to interpret the effect that tilting a structure with cholesteric symmetry, with respect to the electron beam, has on the resultant image.[14] When this twisted plywood model is viewed at an angle, a series of nested arcs, comprising a periodic banding with a larger repeat distance, is observed. A comparison of Figures 6B and 4B* shows this effect schematically and experimentally. The same effect is likewise seen if the microtoming of the cholesteric produces sections which are not taken parallel to the helical axis. Comparison of our diffraction patterns and defocused images to the model of reciprocal space and the twisted plywood model provides a self-consistent explanation for the features observed as a result of changes in the relative orientation of the cholesteric silk structure and the electron beam.

4. Conclusions

Our observations have shown evidence of a cholesteric liquid crystalline phase of silk fibroin in solution. The primary protein structure of silk fibroin has no inherent rigidity, and the mechanism by which these molecules form liquid crystalline phases has not been sufficiently elucidated. Rodlike aggregates of globular or coiled protein chains have been postulated to explain the observation of nematic textures in silk solutions.[5] However, this explanation is incommensurate with our observation of electron diffraction from silk liquid crystal structures. Furthermore, unless the silk protein chains take very specific globular conformations in solution, their aggregates would not be handed and thus would not be able to form the cholesteric twist which we observe. Finally, a liquid crystalline phase of rodlike aggregates of random coils does not achieve orientation on the molecular or segmental level. The presence of such orientation is one of the main reasons to initially postulate a liquid crystalline silk spinning intermediate.

Other candidates for silk liquid crystalline phases are anisotropic secondary or tertiary structures. Due to hydrogen bonding and conformational preferences the silk protein may form secondary structures (helices or β sheets) which have enough shape anisotropy and rigidity to form liquid crystalline phases. These secondary structures are handed objects which are thus likely to favor cholesteric order. The final silk fibroin structure in spun silk fiber is a β-sheet crystal, silk II. We have observed electron diffraction consistent with the silk II structure in the spinneret region of the *B. mori* silk gland.[15] The reported spacings for the diffraction observed with the banded cholesteric textures are very similar to those reported for the silk II structure, but only 100 and *hk*0 reflections are observed, suggesting a lack of crystallographic registry between twisting

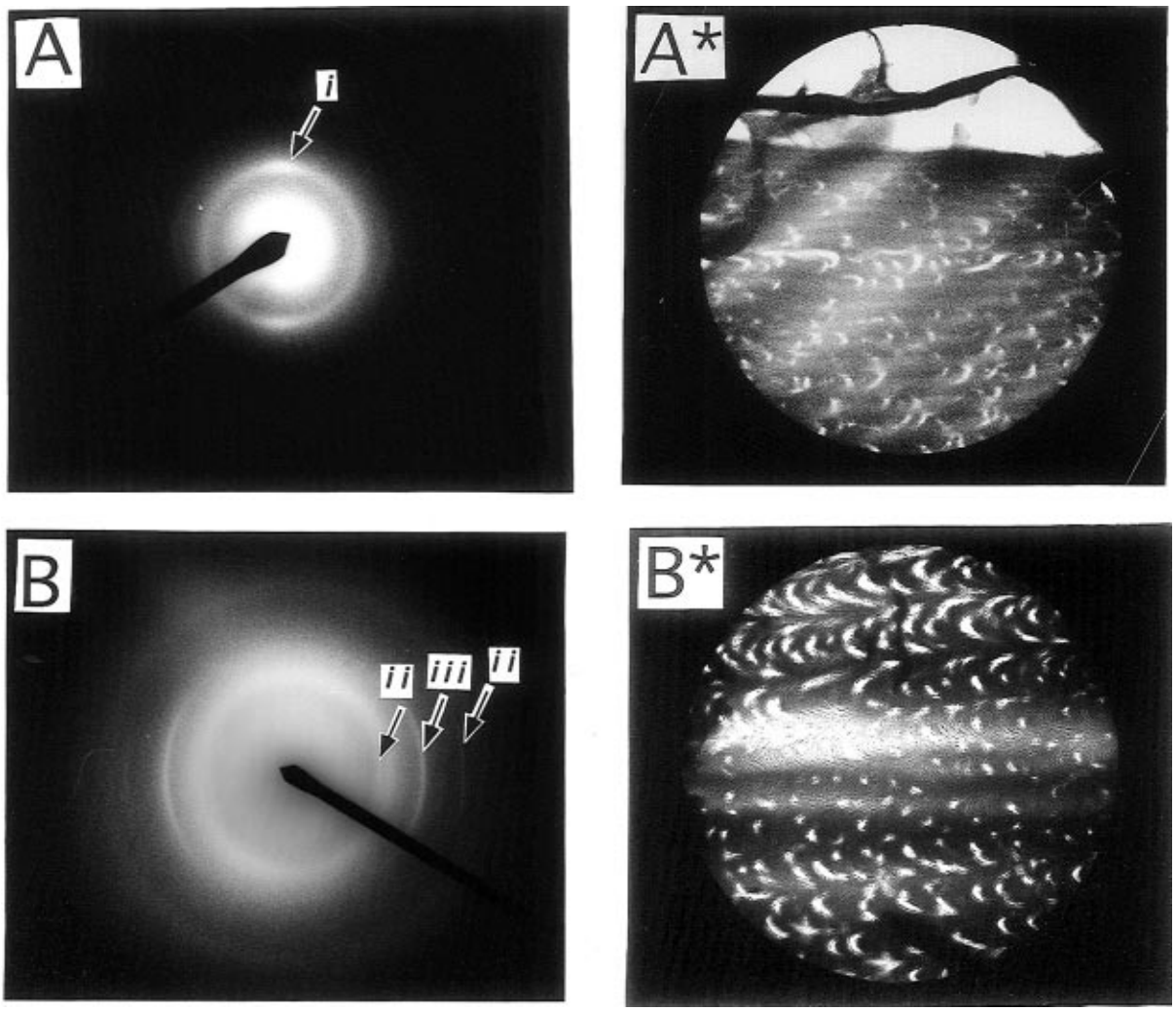

Figure 4. Two sets of electron diffraction patterns and the corresponding defocused images. Approximate molecular repeat distances of (i) 4.70 Å, (ii) 5.20 Å (first order) and 2.60 Å (second order), and (iii) 3.45 Å were obtained for the reflections using an internal gold standard.

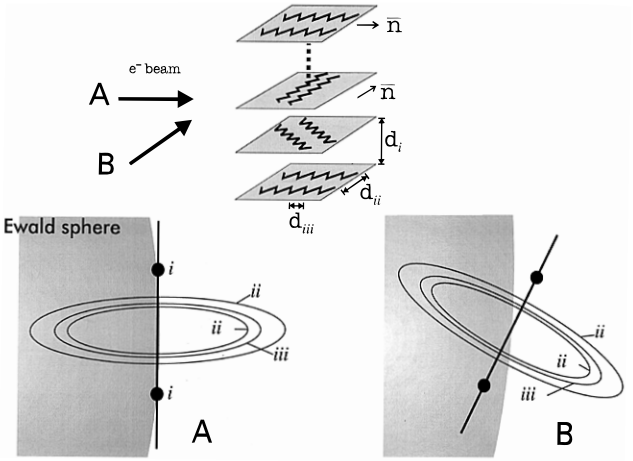

Figure 5. Model representing the geometry for electron diffraction of a cholesteric phase (helically rotating molecular director, *n*): (A) electron beam perpendicular to the axis of twist; (B) electron beam nonperpendicular to the helical axis. The tilt angle affects the intersection of the Ewald sphere and the reciprocal lattice and, consequently, the reflections that are seen in the experiment.

layers (values and index conventions after Marsh *et al.*[16] and Lotz[17]). Therefore, the molecules forming the cholesteric phase may be in the extended chain conformation and very close to assuming their final β-sheet

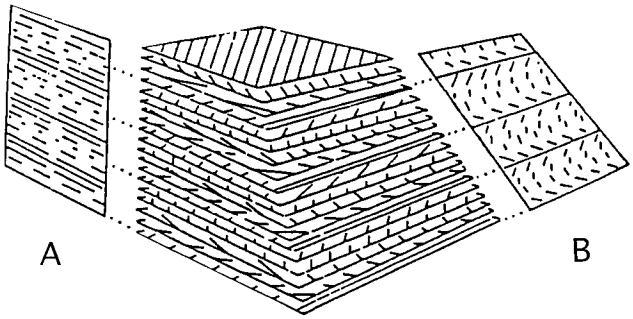

Figure 6. Model of a solid-phase cholesteric as a "twisted plywood".[20] Transverse (A) and oblique (B) sections are shown to illustrate the configuration of the molecules.

crystalline alignment. The transition from a cholesteric structure in the duct to a fully crystalline structure in the spinneret is relatively straightforward to postulate as the mesogenic units orient in the flow direction (i.e., the cholesteric is untwisted to a nematic by flow) and, then, pack into the silk II crystal structure.

The observation of this cholesteric phase of silk is counter to some previous expectations. The postulated liquid crystalline phase of silk was assumed to be nematic, based on the observation of rheological properties such as decreasing viscosity with increasing shear rate along the length of the gland. As a general rule,

such properties are not found in cholesterics. However, a material which forms a cholesteric at equilibrium may be untwisted to a nematic in a flow field.[18,19] If the time scale at which the flow process untwists the cholesteric (reciprocal of the shear rate) is slower than the molecular relaxation time scale, then the cholesteric twist can continuously re-form at a faster rate than it is destroyed. In the silk gland of *B. mori* the shear rate increases along the duct[1] from 2 to 400 s^{-1}. Our sections are taken perpendicular to the flow direction; therefore, our banded texture and diffraction indicate that the helical axis of the cholesteric is perpendicular to the flow direction. If this structure were untwisted by a flow field, the molecules would then be aligned with the flow direction. This orientation is consistent with the alignment of chains along the fiber axis in the spun silk fibers. Also, the repeat distance of our banding, which is equal to 1/2 the pitch of the helical axis,[10] indicates that the twist of this cholesteric phase is weak. The cholesteric may be able to exist in the upper portion of the duct, with a transition to a nematic phase occurring in the flow field of the lower duct. Our TEM observation does not provide a contrast mechanism by which we can observe the nematic. After untwisting to the nematic, the structure then crystallizes to the β-sheet silk II structure which we can observe. We may thus be able to rationalize our observation of a cholesteric structure with previous observations of a nematic in silk solution extracted from the gland and placed between glass surfaces.[4,5] The cholesteric twist is very delicate and may be destroyed by external effects such as flow or surface constraints.

It now remains to more fully define the conformation of the molecule and the conditions within the gland which contribute to this phase of silk.

Acknowledgment. Helpful discussions with D. L. Vezie-Khan, C. Mello, and D. A. Hoagland are acknowledged. Funding was provided through NSF MRSEC for polymers at the University of Massachusetts Amherst, the U.S. Army Research Office (DAAH04-95-1-005), and the W. M. Keck Foundation.

References and Notes

(1) Iizuka, E. In *U.S.−Japan Seminar on Polymer Liquid Crystals*; White, J. L., Onogi, S., Eds.; John Wiley & Sons: New York, 1985; pp 173−186.
(2) Magoshi, J.; Magoshi, Y.; Nakamura, S. *J. Appl. Polym. Sci., Appl. Polym. Symp.* **1985**, *41*, 187−204.
(3) Li, G.; Yu, T. *Makromol. Chem., Rapid Commun.* **1989**, *10*, 387−389.
(4) Kerkam, K.; Viney, C.; Kaplan, D.; Lombardi, S. *Nature* **1991**, *349*, 596−598.
(5) Viney, C.; Huber, A. E.; Dunaway, D. L.; Kerkam, K.; Case, S. T. In *Silk Polymers: Materials Science and Biotechnology*; Kaplan, D., Adams, W. W., Farmer, B., Viney, C., Eds.; American Chemical Society: Washington, DC, 1994.
(6) Sprague, K. U. *Biochemistry* **1975**, *14*, 925−931.
(7) Magoshi, J.; Magoshi, Y.; Nakamura, S. In *Silk Polymers: Materials Science and Biotechnology*; Kaplan, D., Adams, W. W., Farmer, B., Viney, C., Eds.; American Chemical Society: Washington, DC, 1994.
(8) Berreman, D. W.; Meiboom, S.; Zasadzinski, J. A.; Sammon, M. J. *Phys. Rev. Lett.* **1986**, *57*, 1737−1740.
(9) Bouligand, Y. *Tissue Cell* **1986**, *18*, 621−643.
(10) Bunning, T. J.; Vezie, D. L.; Lloyd, P. F.; Haaland, P. D.; Thomas, E. L.; Adams, W. W. *Liq. Cryst.* **1994**, *16*, 769.
(11) Demus, D.; Richter, L. *Textures of Liquid Crystals*; Verlag Chemie: New York, 1978.
(12) Echlin, P. *Low-Temperature Microscopy and Analysis*; Plenum Press: New York, 1992.
(13) Robards, A. W.; Sleytr, U. B. *Low Temperature Methods in Biological Electron Microscopy*; Elsevier: Amsterdam, 1985; Vol. 10.
(14) Livolant, F.; Giraud, M. M.; Bouligand, Y. *Biol. Cell.* **1978**, *31*, 159−168.
(15) Willcox, P. J.; Gido, S. P. To be published.
(16) Marsh, R. E.; Corey, R. B.; Pauling, L. *Biochim.Biophys. Acta* **1955**, *16*, 1−34.
(17) Lotz, B.; Cesari, F. C. *Biochimie* **1979**, *61*, 205−214.
(18) Kiss, G.; Porter, R. S. *J. Polyme.Sci., Polym. Phys. Ed.* **1980**, *18*, 361−388.
(19) De Gennes, P.-G.; Prost, J. *The Physics of Liquid Crystals*, 2nd ed.; Clarendon Press: Oxford, 1993.
(20) Bouligand, Y. *Tissue Cell* **1972**, *4*, 189−217.

MA960588N